Spectrochimica Acta Part A: Molecular and Biomolecular Spectroscopy 226 (2020) 117610

Contents lists available at ScienceDirect

Spectrochimica Acta Part A: Molecular and Biomolecular Spectroscopy

journal homepage: www.elsevier.com/locate/saa

# A fluorescent lateral flow biosensor for the quantitative detection of Vaspin using upconverting nanoparticles

Muhsin Ali [a], Memoon Sajid [a, b], Muhammad Asad Ullah Khalid [a], Soo Wan Kim [a], Jong Hwan Lim [a], Dongeun Huh [c], Kyung Hyun Choi [a, *]

[a] Department of Mechatronics Engineering, Jeju National University, Jeju, South Korea
[b] GIK Institute of Engineering Sciences and Technology Topi, Swabi, KP, Pakistan
[c] Department of Bioengineering, University of Pennsylvania, Philadelphia, PA, 19104, USA

ARTICLE INFO

*Article history:*
Received 9 May 2019
Received in revised form
19 August 2019
Accepted 6 October 2019
Available online 8 October 2019

*Keywords:*
Aptamers
Upconverting nanoparticles
Bioconjugation
Vaspin
Lateral flow biosensor

ABSTRACT

Vaspin is a protein present in human serum that can cause type-2 diabetes, obesity, and other cardiovascular diseases. We report fluorescent upconverting nanoparticles (UCNPs)-based lateral flow biosensor for ultrasensitive detection of Vaspin. A pair (primary and secondary) of cognate aptamers was used that has duo binding with Vaspin. UCNPs with a diameter of around 100 nm were used as a tag to label a detection probe (secondary aptamer). A primary aptamer (capture probe) was immobilized on the test zone. Sandwich type hybridization reactions among the conjugate probe, target Vaspin, and primary aptamer were performed on the lateral flow biosensor. In the presence of target Vaspin, UCNPs were captured on the test zone of the biosensor and the fluorescent intensity of the captured UCNPs was measured through a colorimetric app under NIR. Fluorescence intensity indicates the quantity of Vaspin present in the sample. A range of Vaspin concentration across 0.1−55 ng ml$^{-1}$ with a Limit of detection (LOD) 39 pg ml$^{-1}$ was tested through this UCNPs based LFSA with high sensitivity, reproducibility and repeatability, whereas it's actual range in human blood is from 0.1 to 7 ng ml$^{-1}$. Therefore, this research provides a well-suited lateral flow strip with an ultrasensitive and low-cost approach for the early diagnosis of type-2 diabetes and this could be applied to any targets with a duo of aptamers generated.


## 1. Introduction

Visceral adipose tissue-derived serpin (Vaspin) is considered one of the newest adipocytokine, incorporated with insulin-sensitizing effect [1], it has been potentially associated with obesity, insulin resistance, metabolic syndrome, and type-2 diabetes [2]. Type-2 diabetes mellitus (T2DM) is a nexus metabolic disorder which has influenced more than 150 million people globally and is guessed at to become 439 million worldwide in 2030 [3]. Its prevalence is expected to increase exponentially around the world particularly in developing countries [4]. Level of Vaspin is considerably increased in type-2 diabetes patients as related to normal individuals and further increased in patients with both T2DM and coronary artery disease (CAD). Moreover, Vaspin correlates positively with body mass index, fasting plasma glucose, insulin and Homeostatic model assessment and Insulin resistant (HOMA-IR) in all patients with T2DM ($P < 0.05$) [5,6].

Point-of-care (POC) diagnostic devices are essential in the health safety programs because of identifying the disease biomarkers at the patient site [7,8]. To date, major advances have been accomplished in development of miniaturized and portable devices in the field of healthcare system for immune chromatographic strip (ICS)/lateral flow strip assay (LFSA) which became an imperative technology for the speedy analysis due to its low cost, simple handling, and less conclusion time [9−11]. LFSA was firstly introduced in 1956, which has later been adopted from a logical extension of technology used in latex agglutination test [12] and it can be used at patient site. Lateral flow technology generally avoids the use of standards, data processing, and usually requires the least number of steps depending on the category of POCT, satisfying the acronym "ASSURED" (Affordable, sensitive, specific, user-friendly, robust, equipment free and deliverable to end) [13]. Based on bioreceptors, two types of LFSA have been reported as immunosensors and aptasensor [14]. Furthermore, aptasensor could be generated including target induced displacement [15] and sandwich-type

* Corresponding author.
*E-mail addresses:* memoonsajid@gmail.com (M. Sajid), asadullah967@gmail.com (M.A.U. Khalid), dolage89@naver.com (S.W. Kim), jhlim@jejunu.ac.kr (J.H. Lim), amm@jejunu.ac.kr (K.H. Choi).

https://doi.org/10.1016/j.saa.2019.117610
1386-1425/

assay [16,17]. Sandwich-type is more convenient if the duo aptamers are available for the target analyte which enhances signal generation and improves selectivity. Sandwich-type assay has been rarely reported, probably due to the unavailability of dual aptamers. Though, after the development of aptamers a few sandwich type biosensors have been continuously cited [18–21] resulted in high sensitivity and selectivity. In a recent work, a cognate aptamer duo has also been developed for detection of Vaspin using GO-SELEX process, which has high affinity and selectivity for Vaspin to bind at two different sites on Vaspin [20]. Therefore, sandwich type assay for the detection of vaspin would be followed in the current research work. Furthermore, aptamers have several advantages as a bio recognition elements such as simple synthesis, cheaper, and most importantly, non-immunogenic [22] as compared to antibodies.

On the other hand, nanotechnologies have developed and created an exemplary shift in the field of the biosensors which is one of the most well-known methods of diagnostics, clinical analysis, and environmental monitoring [23]. A great alternative to counterfeit the difficulties of sensitivity associated with colorimetric detection, fluorescent nanoparticles could be used. Fluorescent based various biosensors and chemosensors have been developed [24–26] using AIE active molecules and are promising for biomedical applications [27–29]. Highly sensitive optical-based biosensor requires fluorescent bio label which can give quantitative results such as DNA biosensor [30] tetrodotoxin [31] and $Hg^{2+}$ [32]. Up-converting nanoparticles (UCNPs) based aptasensor can be developed for the detection of Vaspin [33]. At present, UCNPs have been used to detect hepatitis B [34], Brucella [35], Schistosoma circulating anodic antigen [36], interferon-γ (IFN-ɣ), cTnI and PSA, and target-DNA resulting in higher sensitivities. UCNPs have the advantages of being biocompatibility, stable results, low background light, high sensitivity, and most importantly low cost and no bleaching effects and blinking unlike many quantum dots [37]. On the basis of its crystal shape, it has been proved that hexagonal crystals have strong up-conversion efficiency as compared to cubic shape [5,38–40]. Till now, colorimetric based detection of Vaspin has been reported only by using gold nanoparticles (AuNPs) with a detection limit of 0.137 nM [41]. Optical signals of AuNPs may not be as strong as fluorescent nanoparticles. It also results in a process which could be reversed by changing the condition that influences the strength of the interaction (e.g. pH, and polarity of the solvent). This approach limits to desorption of bioconjugation which hinders the reproducibility. The reproducibility of the proposed biosensor has not been discussed in their research which is a parameter of great significance in the field of biosensors along with repeatability, and is quite challenging. Physical adsorption of biomolecules to the surface of UCNPs is possible. However, covalent linkage is preferred in order to prevent desorption and increase the conjugate stability in a wide range of sample matrices. It results in higher specificity, sensitivity, and reproducibility that can be used for quantitative analysis not only qualitative detection, thus making it more appropriate for POCT devices.

In light of all the above discussion, we have developed a fluorescent based LFSA for vaspin. UCNPs conjugation with secondary aptamers has been established which has the potential for enhanced sensitivity, reproducibility, stable fluorescence, low cost nanoparticles, and quantitative results of Vaspin as contrary to its counterpart based on AuNPs. The quantity of Vaspin present in the serum can provide critical information about the mentioned diseases using a relatively simple and easy procedure. As per our knowledge, this is the first report of fluorescence based LFSA for the quantitative detection of vaspin using covalently bounded conjugates. This LFSA is so far the most sensitive method reported for the rapid detection of Vaspin without the additional signal amplification and use of conventional fluorescence dyes. This LFSA can detect Vaspin in the human serum in the range of nanomolar concentrations. The promising properties of the UCNPs conjugate analyzed are reported below.

## 2. Experimental section

### 2.1. Apparatus

The following instruments were used for the characterization of materials: Raman spectroscopy (Lab RAM HR Raman) with a solid-state laser at room temperature with the excitation laser wavelength of 514 nm; FTIR (Nicolet 6700 FT-IR spectrophotometer); Photoluminescence spectroscopy (LS-55 PerkinElmer Fluorescence Spectrometer) ranging from 200 nm to 800 nm; Transmission electron microscope (JEOL JEM-2010 operated at 200 kV with $LaB_6$ electron gun); High-performance X-ray Photoelectron Spectrometer; Particle Size Analyzer and Guillotine cutting module for strip cutting. Mortar and pestle was used for grinding purposes. A CW diode laser (980 nm) setup was used for the excitation of UCNPs and was observed by using an android phone for quantitative analysis of Vaspin through a colorimetric app.

### 2.2. Materials

Cellulose fiber sample pad (CFSP203000, 20 × 300 mm) and Hi-flow NC membrane (HF090MC100, 60 × 300 mm) were purchased from the Sure Wick and Hi-flow plus company respectively. For assembling the respective pads on support, baking cards were ordered from DCN. UCNPs ($NaYF_4$: 20 mol%Yb, 2 mol%Er), streptavidin, BSA, and Tween 20 were purchased from Sigma Aldrich. Mal-PEG-COOH (1000) was purchased from NANOCS and Vaspin was procured from Adipogen. The details of all the DNA oligonucleotides (aptamers) used in this study are provided in Table S1, that were selected by using SELEX process [20] and were acquired from Genotech company Korea. All the chemicals used in this study were analytical reagent grade.

### 2.3. Particle size reduction

$NayF_4$: Yb, Er (20 mol%, 2 mol %) up-conversion particles were ordered from Sigma Aldrich which have been synthesized by hydrothermal/salvo process having a coating of oleic acid. The sizes of the particles were reduced in mortar and pestle by grinding them for 4 h. A colloidal solution was then made in ethanol to be further processed by ultrasonic probe sonication. Subsequently, the solution was centrifuged at 8000 rpm and the supernant was separated to obtain reduce size particles.

### 2.4. Ligand exchange of UCNPs with Mal-PEG-COOH

For covalent linkages, the surface of UCNPs has to be functionalized with appropriate (maleimide) functional group in order to bind with the biomolecule functional group (thiol) [42,43]. Ligand exchange of UCNPs was performed according to the previous report with customization. Approximately 5 mg of oleic acid coated UCNPs were added to 50 mg of Mal–PEG–COOH (1000) dissolved in 500 μl ethanol. The solution was kept in an Argon atmosphere and was shaken in a thermomixer (1000 rpm) for 48 h at 40 °C. To precipitate the UCNPs coated with Mal–PEG–COOH, hexane was added to the mixture. The nanoparticles were isolated through centrifugation and washed with ethanol. Finally, a dispersion of 1 mg $ml^{-1}$ of the nanoparticles in ethanol was stored at 4 °C under slow rotation. Before the coupling reaction with thiolated aptamer (secondary aptamer), ethanol was removed by centrifugation (4000 rpm) and was replaced by PBS. Functionalization can also be done by salinization but it aggregates after reacting with biomolecules [44].

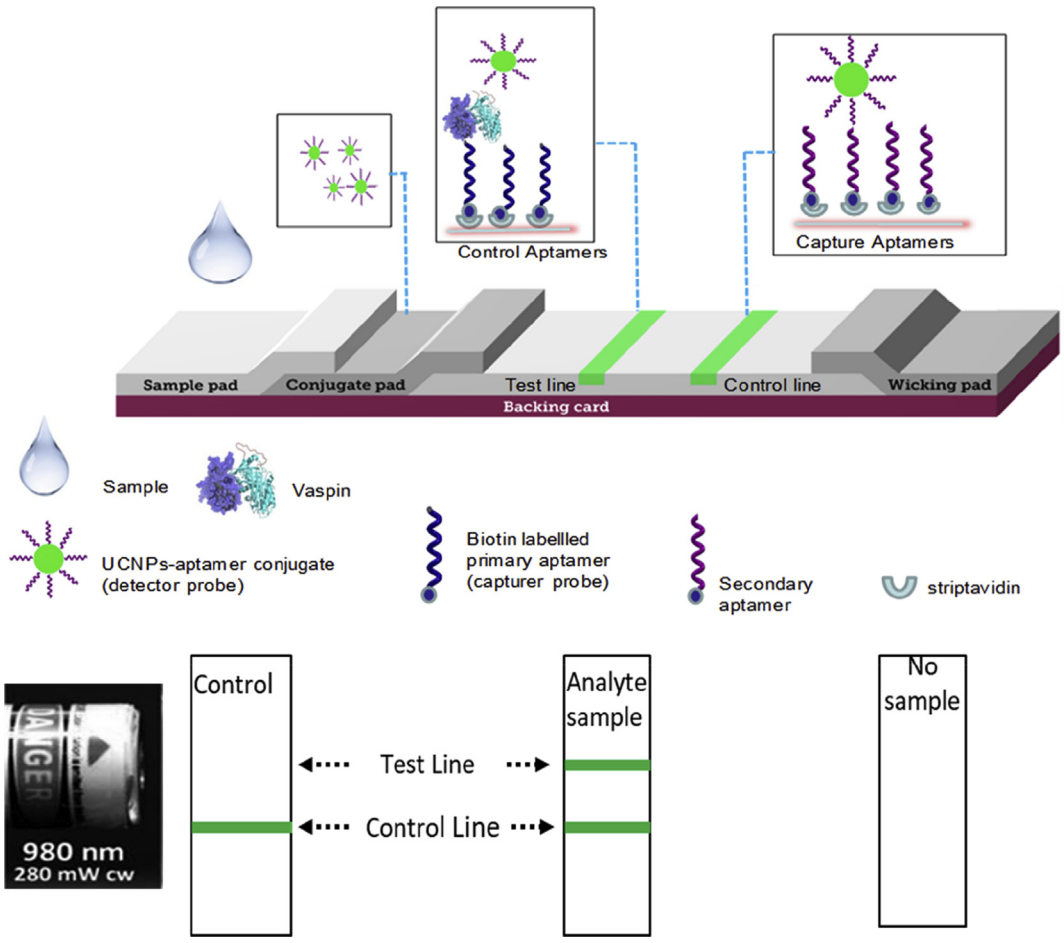


**Fig. 1.** Schematic illustration of the configuration of the UCNPs based lateral flow vaspin sensor and principle of qualitative detection of vaspin on the fluorescent upconverting nanoparticles based lateral flow biosensor.

### 2.5. Bioconjugation (Aptamers/UCNPs)

Aptamers are short oligonucleotides having the capability to bind to a specific target-oligonucleotide analyte (VASPIN) [45]. A new labeling strategy has been developed to conjugate the thiolated aptamer with the functionalized UCNPs as shown in Fig. S1. The thiol group of the secondary aptamer reacts with the double bond of maleimide to form a carbon-sulfur bond (thioether bond formation). The modified UCNPs were provided with long PEG chains which will be reducing the unspecific binding. So the 500 μl maleimide activated UCNPs and 26 μl secondary aptamer-SH (10 nM) were mixed in PBS (pH = 7.4). After 24 h reaction at 4 °C, excess aptamers were removed by centrifugation, and the resultant UCNP-PEG-aptamers was re-suspended in PBS and stored at 4 °C for further experiments.

### 2.6. Lateral flow strip

A lateral flow strip consists of three main overlapping pads assembled on laminating/baking card as a support. Sample application pad was made of cellulose fiber (CFSP203000, 20 × 300 mm). The UCNPs-aptamer (detection probe) conjugate solution was dispensed on the glass fiber conjugate pad through micro liter pipette. To aid the immobilization of biotin-capture primary aptamer and biotin-capture control aptamer probes, streptavidin (0.5 mg $ml^{-1}$, 30 μl) was dispensed on test line and control line before dispensing the aptamers solutions, to react with and form stable conjugates, incubated for 1 h at 4 °C. Aptamer solutions were dispensed on NC membrane to form the test and control line. After dispensing, the conjugate and cellulose membranes were dried at 37 °C for 2 h before assembly. 0.5–1% trehalose was added to striping solution to increase the stability of the protein binding on the membrane. Test and control lines are 1 mm wide and 5 mm apart as shown in Fig. 1. The minimum overlapping distance between the sample and conjugate pad was kept to avoid developing dead space which then serves as a reservoir for slower conjugate release. Subsequently, PBS buffer containing BSA (50 μg $ml^{-1}$) was run through the membrane in order to reduce the matrix interpretation and increase the signal-to-noise (S/N) ratio through blocking. To assemble on the laminate baking card (ordered from DCN), the nitrocellulose was applied first, followed by the conjugate pad, wicking pad, and then sample pad. The control line exhibited successfully captured Vaspin free aptamer conjugate, showing that the reaction conditions and assay worked fine.

### 2.7. Sample assay procedure

Under the optimized experimental conditions, the performance of the UCNPs LFSA was evaluated with different concentrations of target Vaspin in the running buffer, PBS (pH~7.0) + 0.5% BSA. In a typical assay 50 μl of the sample solution was introduced to the sample pad as shown in Fig. 1; the solution then migrated towards absorption pad by the capillary force. The fluorescence images of the test zone and control zone were evaluated visually under near-infrared CW laser diode (980 nm) which gives fluorescence in the visible range. The smartphone was located on self-made detector

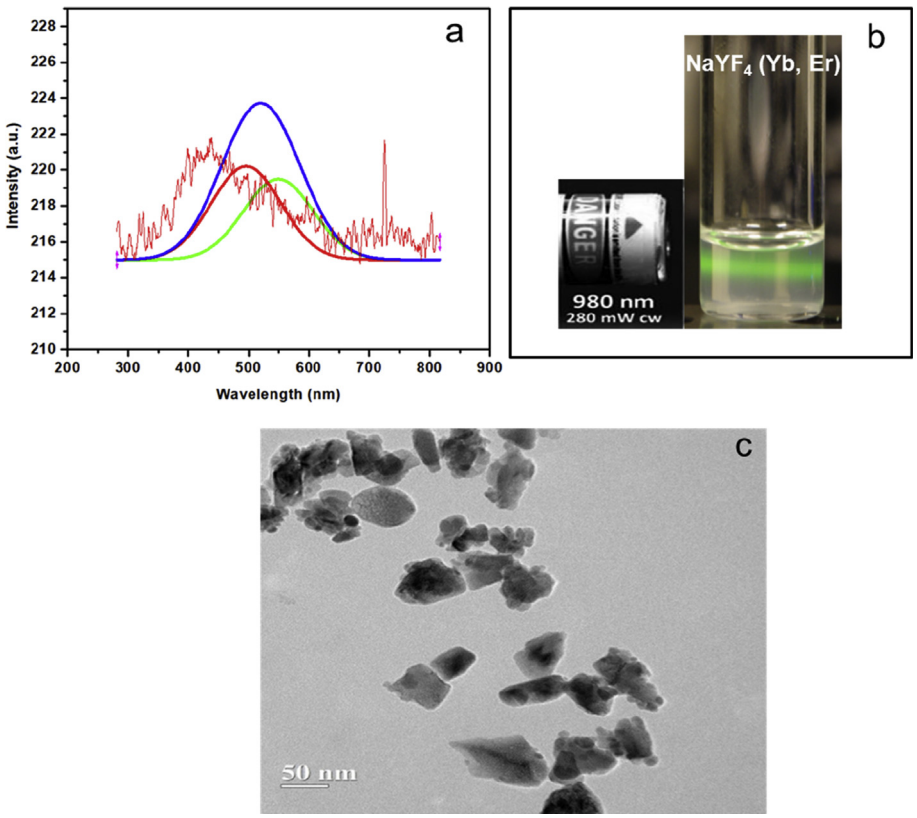


**Fig. 2.** (a) Photoluminescence spectroscopy of the colloidal solution of the UCNPs under excitation wavelength of 980 nm **(b)** Fluorescence of nanoparticles colloidal solution (5 mg ml$^{-1}$) **(c)** TEM images of $NaYF_4$ (Yb: Er) nanoparticles.

holder and images were collected in a dark box to avoid the effect from surrounding light for quantitative analysis. The fluorescent intensities of the test line and control line were recorded by using the mobile phone camera to calculate RGB values through a colorimetric app as shown in Fig. S2. Only the change in intensity of the green coordinate was considered on test line to translate the amount of analyte into a detectable changing entity. The ability of the sensor was tested for the target Vaspin in buffer samples. A variety of known concentrated samples were prepared and tested. A linear calibration curve was obtained for the intensity of green color coordinate vs the quantity of known analyte present in the sample. The system was then tested to calculate three known concentrations of Vaspin in independent samples within clinical range, solely using the calibration curve and the fluorescence intensity.

## 3. Results and discussions

### 3.1. Fluorescent nanoparticles

1 μm size particles were grounded to get nanometer size particles; they were characterized using TEM to confirm the particle size reduction. Fig. 2(c) shows the reduced particles of oleic acid capped $NaYF_4$: 20 mol% Yb, 2 mol% Er. They have an average size under 100 nm and quantum yield of 3% [46]. DLS measurement has also shown in Fig. S5. The fluorescent properties were tested using photoluminescence spectroscopy to approve that the excitation/emission wavelength remains unaffected. Fig. 2(a) shows the Gaussian fitting and photoluminescence (PL) emission spectra of UCNPs. It shows the deconvoluted peaks at different wavelengths, at 550 nm (green line) indicating the emission of green fluorescence when excited under a CW laser of 980 nm. The other related peaks were also observed which may be associated with the change in lattice strain after reduction of particle size. The overall color output appears green which dominates the red emission [42]. The results were further cemented by exciting a liquid sample of the nanoparticles under a near infra-red (NIR) 980 nm laser excitation source of power 30 mW. Fig. 2(b) shows the image of the visible green emission. XPS measurement of UCNPs has shown in Fig. S4.

### 3.2. Functionalization and conjugation

Raman spectroscopy was used to detect the maleimide group indirectly because the peak for maleimide was pretty indistinct in the whole spectrum. The surface of nanoparticles was modified by ligand exchange process using PEG; the ether group (R-O-R) is responsible for it which has a symmetric stretching vibration in the range of 800–920 cm$^{-1}$ that can be confirmed from Fig. 3(b) having peaks at 793, 880 and 926 cm$^{-1}$ respectively [44]. These peaks are usually absent for the UC control and modified nanoparticles using salinization method. Therefore, usually the Raman spectra of UCNPs@$SiO_2$—PEG-Mal and UCNP@$SiO_2$ contains no PEG and hence serves as a control in the region between 700 and 1000 cm$^{-1}$ [47]. UCNPs@Mal-PEG show specific Raman bands with a maximum of 850 cm$^{-1}$ or 855 cm$^{-1}$ subsequently, which can be accredited to the symmetric stretching vibrations of the PEG ether group (R-O-R) on the UCNPs surface. This Raman band is absent in UCNP@$SiO_2$ without PEG-modification [47]. It concludes that oleic acid capped nanoparticles were successfully converted to maleimide functional group by PEG. The complete Raman spectrum from 100 to 1000 cm$^{-1}$ is presented in Fig. 3(c) which confirms that the surface of oleic acid capped nanoparticles has been exchanged by maleimide group through ligand exchange process as there are no stretching vibrations between 200 and 400 cm$^{-1}$. For control of

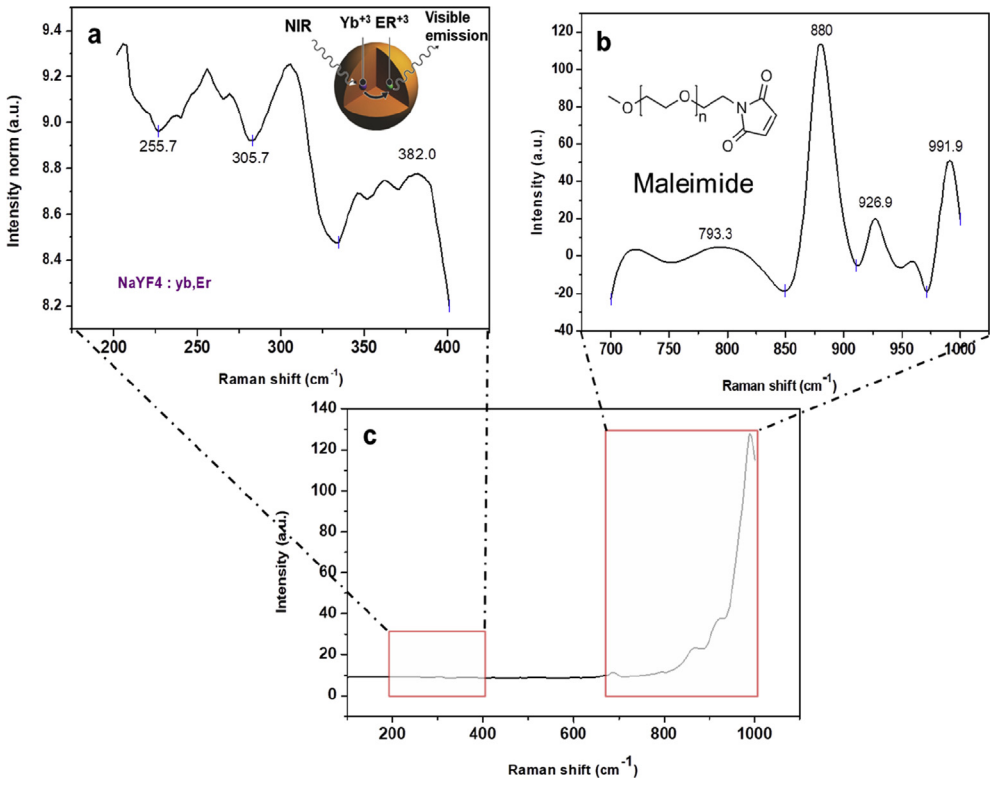


**Fig. 3. Raman spectra of UCNPs (a)** Spectra of 100 nm unmodified upconverting nanoparticles $NaYF_4$ (Yb: Er) **(b)** UCNPs@Mal-PEG-COOH modified particles showing the characteristics stretching of ether group (R-O-R) between 800 and 920 $cm^{-1}$ **(c)** Complete Raman spectrum of the functionalized particles.

characterized unmodified UCNPs spectrum band [48] has been shown in Fig. 3(a).

Bioconjugation (Coating of thioled functional secondary aptamer onto the surface of maleimide functionalized UCNPs) was further verified by FT-IR analysis. Binding of the thiol group of the aptamer with maleimide functionalized UCNPs was made sure as shown in Fig. 4 that could also be used to analyze the stability. In case of OA capped UCNPs the bands at 1454 and 1546 $cm^{-1}$ accredited to the asymmetric (υas) and symmetric (υs) stretching vibrations of the −COOH- group of oleic acid. The transmission bands at around 2848 and 2924 $cm^{-1}$ are attributed to the asymmetric and symmetric stretching vibrations of C—H in the alkyl chain from oleic acid molecule, and the band at around 3426 $cm^{-1}$ attributed to = C—H— stretching vibration in the prepared sample. In the same manner after the conjugation of OA capped nanoparticles can be confirm either by the appearance of new absorption bands in the IR spectra. Here the main concerned band is 1646 $cm^{-1}$. The main bond of concern here is the thioether bond which owe to the covalent bond between maleimide functional group of nanoparticles and thiol group of the aptamer and the typical signal arise at 1646 $cm^{-1}$ made sure the bioconjugation. These observations show indication of successful fabrication of bioconjugation.

### 3.3. Vaspin detection using fluorescent LFSA

The lateral flow strip was fabricated for detection of Vaspin. Biotin-labeled aptamer (capturing probe) was incubated with streptavidin for adjustment on the surface of the membrane (Test line). Simultaneously, the complementary sequence of secondary aptamer was bound to streptavidin for the alignment on the surface of the membrane (control line). Sample pad has been used for the sample introduction. Conjugate pad was deposited with UCNPs aptamer conjugate, working as a detection probe. FTIR spectrum of UCNPs conjugate is showing in Fig. 3 representing the existence of thioether (maleimide + thiol) bond between secondary aptamer and UCNPs. Upon the introduction of the sample, the labeled aptamer on conjugate pad bound to epitope of Vaspin, whereas primary aptamer on the test line captured the other site of the Vaspin (sandwich assay) while passing on. The target free aptamer was seized by control line which could always be observed as a control. Upon excitation to the near infrared zone, the UCNPs gave fluorescence on both test and control zones which confirms the presence of Vaspin and intensity of fluorescence facilitates its quantitative information.

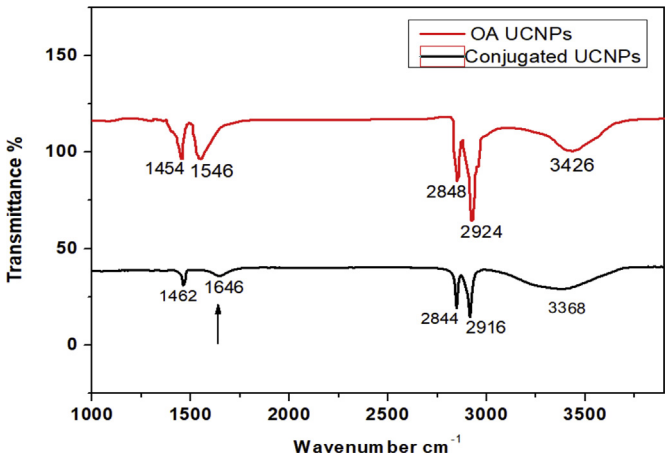


**Fig. 4. FTIR spectrum of the aptamer-UCNPs conjugate:** different peak positions confirming the presence of upconverting nanoparticles ($NaYF_4$: Yb, Er) and oligomers (Aptamer).

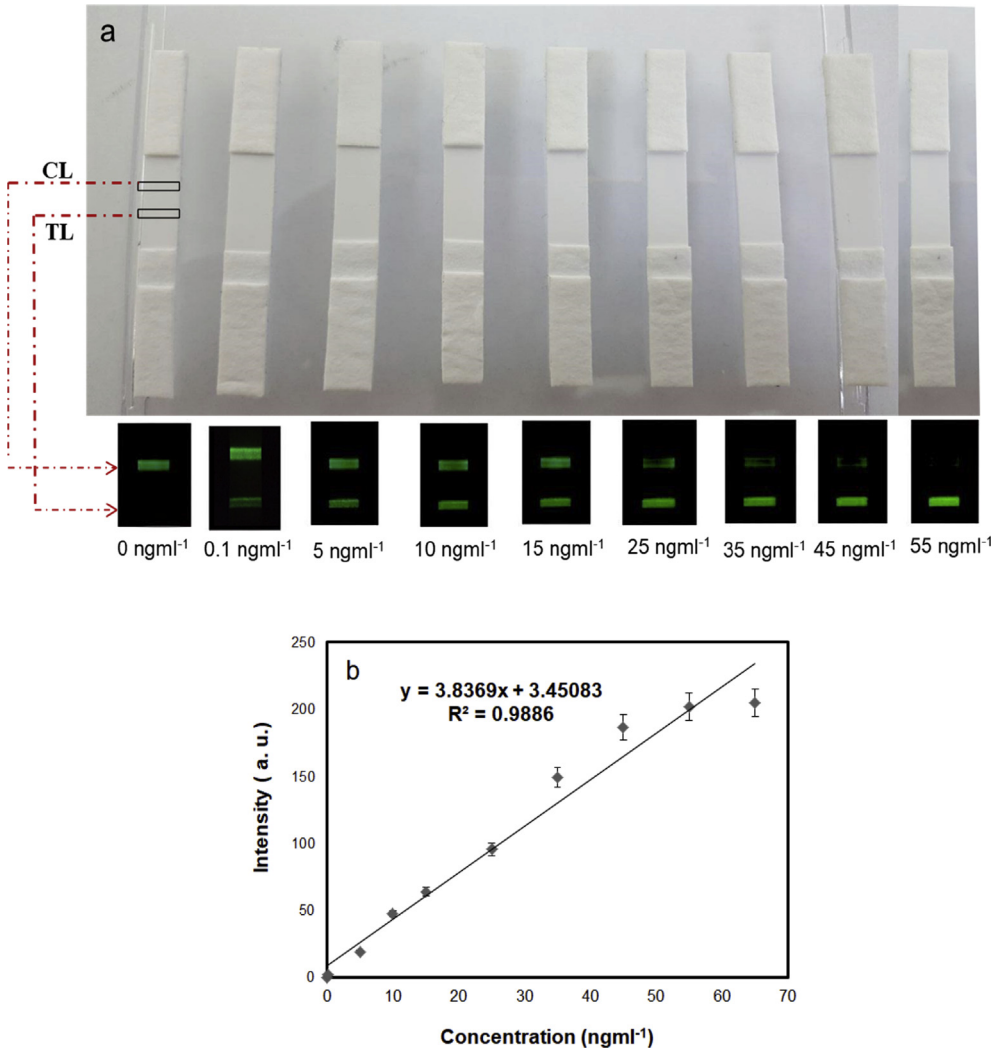


**Fig. 5. Analysis of LFSA (a)** Images of the sensor with different concentrations of target Vaspin under the optimal experimental conditions and **(b)** Calibration curve of test line intensity versus Vaspin concentration. Error bars represent standard deviation, n = 3.

Under optimized experimental conditions, the performance of LFSA was tested in the presence of different target vaspin concentrations. The captured vaspin on the test line was observed visually under NIR and the fluorescence intensity of the test line was measured to quantify the target concentration. A series of the increased intensity test zones were observed with increasing target Vaspin concentrations indicating the good reliability of the strip within a suitable concentration ranges. The resulting curve of the

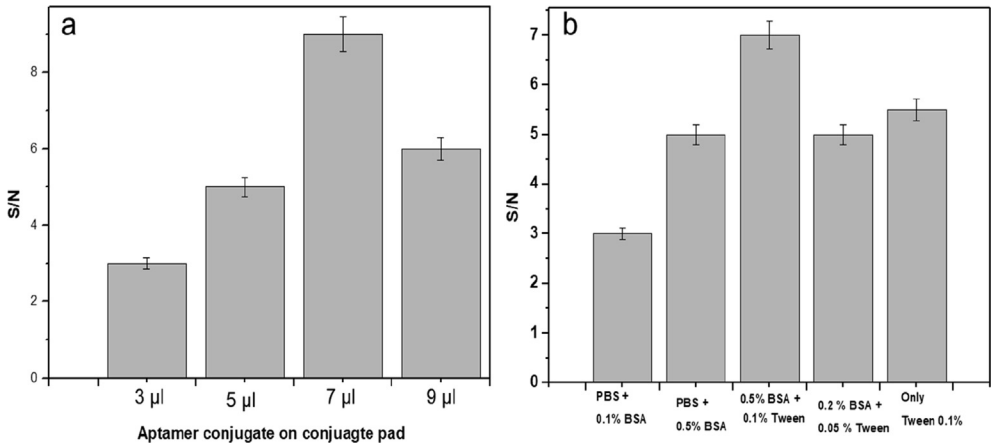


**Fig. 6.** (a) Effect of the volume of UCNPs aptamer conjugate on conjugate pad of LFSA (b) effect of running buffers to increase the flow on UCNPs based LFSA.

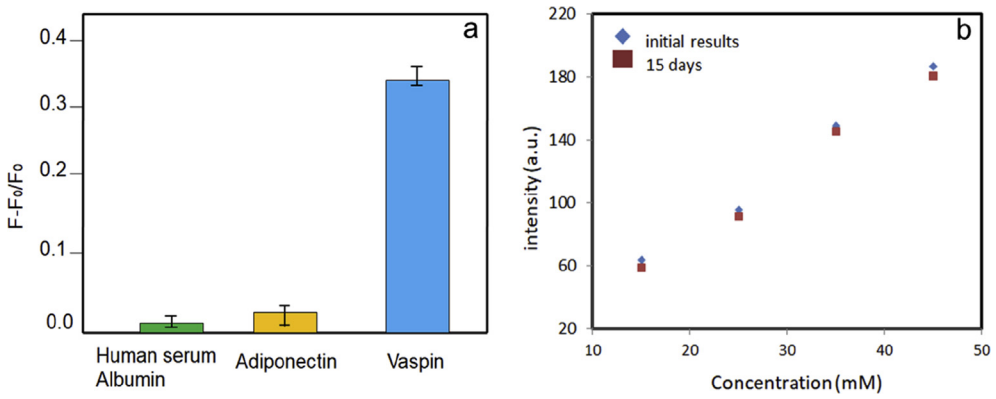


**Fig. 7.** **(a)** Selectivity of the aptamer duo UCNPs conjugate based LFSA for Vaspin with other counter targets such as human serum albumin and Adiponectin (b) reproducibility of LFSA.

target Vaspin versus the fluorescence intensity was almost linear over a range of 0.1–55 ng ml$^{-1}$ with a detection limit of 39 pg ml$^{-1}$ and $R^2 = 0.9886$ as shown in Fig. 5. The assay time is around 2–3 min. The detection limit of UCNPs conjugate in this report is 16 times greater than that of AuNPs based detection of Vaspin (LOD = 0.137 nM) without signal amplification. The benefits of the proposed method in this report include: lower cost than the AuNPs, low limit of detection, highly repeatable results, high stability due to covalent linkages, and reproducibility along with quantitative results.

The sample glided from the sample pad through cellulose membrane towards the wicking pad (to absorb the matrix in the sample). As shown in Fig. 1, signal could be observed only in the presence of Vaspin. The amount of aptamer-UCNPs conjugate must be higher enough than the amount of aptamers on test line and control line. In this study, the amount of conjugate was calculated to be greater than the highest concentration of Vaspin (55 ngml$^{-1}$) which is much higher than the normal concentration in the human blood (0.1–7 ngml$^{-1}$). Therefore, it should be shared with both test and control line. The saturation of test line occurred after 55 ngml$^{-1}$ and the linear range leads to constant observation. In order to develop a point of care testing device for vaspin, the developed strip was evaluated to confirm the uninterrupted vaspin target, specifically 0.8 μgml$^{-1}$ Vaspin, Adiponectin and human serum albumin were assayed as shown in Fig. 6. Before loading the sample, strips were pretreated with PBS and 0.1% Tween 20 to increase the wettability. 50 μl sample was introduced to each prepared strip and fluorescence of UCNPs was recorded.

### 3.4. Optimization of experimental parameters

To obtain the maximum vaspin detection using the UCNPs based LFSA, amount of conjugate on the conjugate pad and running buffers on the strip were optimized. The effect of running buffer on the strip has been considered as one of the most important parameter in the optimization of lateral flow assay. Appropriate pretreatment with different concentrations of BSA and Tween has been analyzed to reduce the nonspecific adsorption and increase the sensitivity and reproducibility of the proposed assay. As shown in Fig. 6(a), the highest S/N ratio was obtained by using 0.5% BSA +0.1% Tween. The amount of UCNPs conjugate aptamer is related to the intensities of test and control lines respectively. As shown in Figs. 6(b) and 7 μl of conjugate has shown highest S/N ratio which was used as the optimal volume dispensed on conjugate pad.

### 3.5. Specificity and stability assessment of the LFSA

To evaluate the specificity of the aptamer-based fluorescence biosensor for Vaspin, the effect of two other analytes which are involved in regulating glucose level and often appear in serum; Human serum albumin and Adiponectin (0.8 μg ml$^{-1}$ each), were examined in aqueous buffer. As shown in Fig. 7, none of these analogs caused obvious changes in the fluorescence while a significant fluorescence change was observed for the Vaspin of the same concentration 0.8 μg ml$^{-1}$. This outcome has thus clearly demonstrated that the designed LFSA has a high specificity for the Vaspin. Besides specificity, stability of the biosensor was also investigated. As predictable, no clear change was spotted after 15 days of biosensor storage at 4 °C. Therefore, the high selectivity and stable detection for Vaspin could be ensured by this rapid LFSA biosensor based on UCNPs.

### 3.6. Detection in serum samples

To examine the practicality of the proposed assay in real samples, the applicability and anti-interference ability of target Vaspin in spiked human serum samples which are a complex biological

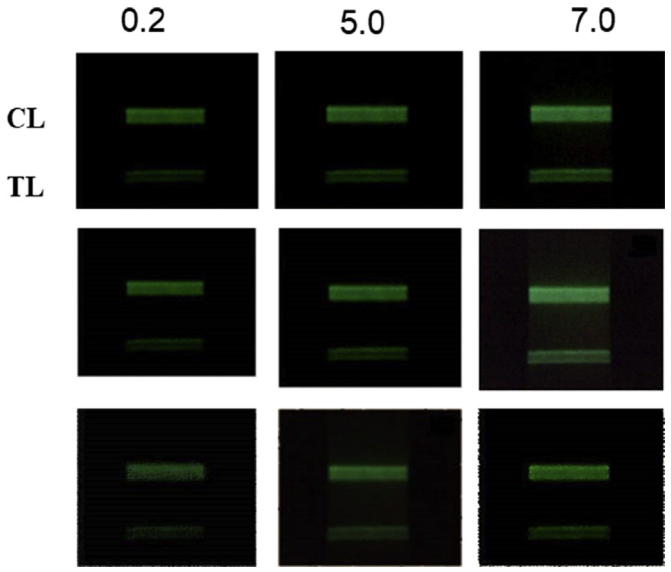


**Fig. 8.** Detection of Vaspin spiked in human serum (pH = 7.0) using UC based LFSA, different concentration of vaspin were diluted in serum samples and observed under exication of 980 nm laser.

fluid containing a variety of matrices present, using the proposed method was studied. In this study three known concentrations of target Vaspin (0.2, 5, and 7 ng ml$^{-1}$) were spiked in human serum samples and evaluated 3 times each concentration for the reproducibility of the biosensor. The serum samples were diluted to 3.5% PBS. The same concentrations and the fluorescence intensities of test line were measured. The system returns values within ranges of 98%, 101% and 96% of the known amounts for 0.2, 5, and 7 ng ml$^{-1}$ targets respectively as shown in Fig. 8. This indicates a very good reproducibility and high potential to develop an assay for future clinical applications.

Recovery results of Vaspin detection in serum (n = 3).

| Added concentration (ng ml$^{-1}$) | Fluorescence Intensity (a.u.) | Detected concentration (ng ml$^{-1}$) | Recovery Ratio (%) |
|---|---|---|---|
| 0.2 | 1.5 | 0.19 ± 0.21 | 98.1 |
| 5.0 | 17.8 | 4.89 ± 0.13 | 101 |
| 7.0 | 23.1 | 7.12 ± 0.09 | 96.9 |

## 4. Conclusion

UCNPs were first used as a tag to develop a lateral flow biosensor for ultrasensitive and quantitative detection of Vaspin (pre-diagnosis biomarker for type-2 diabetes). Secondary aptamers have been specifically and covalently conjugated on the UCNPs surface. Under the optimum conditions such as conjugate volume and running buffer, this LFSA was capable in detecting a minimum of 39 pg ml$^{-1}$ Vaspin in the sample without any additional signal amplification. Vaspin has been detected in both buffer (0–55 ng ml$^{-1}$) and serum (0.2, 5, and 7 ng ml$^{-1}$) conditions. The obtained maleimide-functionalized UCNPs exhibited the best results of low agglomeration by ligand exchange method, and readily reacted with the thiolated aptamers. Further, the use of bioconjugation instead of physical adsorption showed comparatively much higher specificity, reproducibility and facilitated quantitative detection instead of qualitative analysis for Vaspin. To consider the intense fluorescence of UCNPs, further work will aim to develop a multiplex sensor for multiple analytes in the same sample using different colored UCNPs. The UCNPs based LFSA in this work shows excellent results with stable response, rapid and sensitive detection of Vaspin, particularly in limited resource settings.

## Declaration of competing interestCOI

The authors declare no competing interests.

## Acknowledgement

The research was supported by the Program of National Research Foundation of Korea through the Ministry of Education.

## Abbreviations

LFSA Lateral flow strip assay
VASPIN Visceral adipose tissue derived serpine
Mal-PEG-COOH Maleimide polyethylene glycol carboxyl
TL and CL Test line and control line
POCT Point of care testing
UCNPs Upconverting nanoparticles
BSA Bovine serum Albumin
HSA Human serum albumin
T2DM Type 2 diabetes mellitus
CAD Coronary artery disease
CTnI Troponin I
PSA Prostate specific antigen
TEM Transmission electron microscopy
HOMA and IR Homeostatic model assessment and Insulin resistant

## Appendix A. Supplementary data

Supplementary data to this article can be found online at https://doi.org/10.1016/j.saa.2019.117610.

## References

[1] A. Salek-Maghsoudi, F. Vakhshiteh, R. Torabi, S. Hassani, M.R. Ganjali, P. Norouzi, M. Hosseini, M. Abdollahi, Recent advances in biosensor technology in assessment of early diabetes biomarkers, Biosens. Bioelectron. 99 (2018) 122–135.
[2] K. Kempf, B. Rose, T. Illig, W. Rathmann, K. Strassburger, B. Thorand, C. Meisinger, H.-E. Wichmann, C. Herder, C. Vollmert, Vaspin (SERPINA12) genotypes and risk of type 2 diabetes: results from the MONICA/KORA studies, Exp. Clin. Endocrinol. Diabetes 118 (2010) 184–189.
[3] H.O. El-Mesallamy, D.H. Kassem, E. El-Demerdash, A.I. Amin, Vaspin and visfatin/Nampt are interesting interrelated adipokines playing a role in the pathogenesis of type 2 diabetes mellitus, Metab. Clin. Exp. 60 (2011) 63–70.
[4] H.O. El-Mesallamy, D.H. Kassem, E. El-Demerdash, A.I. Amin, Vaspin and visfatin/Nampt are interesting interrelated adipokines playing a role in the pathogenesis of type 2 diabetes mellitus, Metabolism 60 (2011) 63–70.
[5] F. Hao, H. Zhang, J. Zhu, H. Kuang, Q. Yu, M. Bai, J. Mu, Association between vaspin level and coronary artery disease in patients with type 2 diabetes, Diabetes Res. Clin. Pract. 113 (2016) 26–32.
[6] R. Feng, Y. Li, C. Wang, C. Luo, L. Liu, F. Chuo, Q. Li, C. Sun, Higher vaspin levels in subjects with obesity and type 2 diabetes mellitus: a meta-analysis, Diabetes Res. Clin. Pract. 106 (2014) 88–94.
[7] B. Srinivasan, S. Tung, Development and applications of portable biosensors, J. Lab. Autom. 20 (2015) 365–389.
[8] A. Dhiman, P. Kalra, V. Bansal, J.G. Bruno, T.K. Sharma, Aptamer-based point-of-care diagnostic platforms, Sens. Actuators B Chem. 246 (2017) 535–553.
[9] Y. Na, W. Sheng, M. Yuan, L. Li, B. Liu, Y. Zhang, S. Wang, Enzyme-linked immunosorbent assay and immunochromatographic strip for rapid detection of atrazine in water samples, Microchimica Acta 177 (2012) 177–184.
[10] X. Wang, K. Li, D. Shi, N. Xiong, X. Jin, J. Yi, D. Bi, Development of an immunochromatographic lateral-flow test strip for rapid detection of sulfonamides in eggs and chicken muscles, J. Agric. Food Chem. 55 (2007) 2072–2078.
[11] C.I. Justino, A.C. Freitas, R. Pereira, A.C. Duarte, T.A.R. Santos, Recent developments in recognition elements for chemical sensors and biosensors, Trac. Trends Anal. Chem. 68 (2015) 2–17.
[12] J.M. Singer, C.M. Plotz, The latex fixation test: I. Application to the serologic diagnosis of rheumatoid arthritis, Am. J. Med. 21 (1956) 888–892.
[13] J. Sun, Y. Li, F. Pi, J. Ji, Y. Zhang, X. Sun, Using fluorescence immunochromatographic test strips based on quantum dots for the rapid and sensitive determination of microcystin-LR, Anal. Bioanal. Chem. 409 (2017) 2213–2220.
[14] V. Crivianu-Gaita, M. Thompson, Immobilization of Fab'fragments onto substrate surfaces: a survey of methods and applications, Biosens. Bioelectron. 70 (2015) 167–180.
[15] L. Wang, W. Ma, W. Chen, L. Liu, W. Ma, Y. Zhu, L. Xu, H. Kuang, C. Xu, An aptamer-based chromatographic strip assay for sensitive toxin semi-quantitative detection, Biosens. Bioelectron. 26 (2011) 3059–3062.
[16] M. Sajid, A.-N. Kawde, M. Daud, Designs, formats and applications of lateral flow assay: a literature review, J. Saudi Chem. Soc. 19 (2015) 689–705.
[17] H. Xu, X. Mao, Q. Zeng, S. Wang, A.-N. Kawde, G. Liu, Aptamer-functionalized gold nanoparticles as probes in a dry-reagent strip biosensor for protein analysis, Anal. Chem. 81 (2008) 669–675.
[18] V.-T. Nguyen, H.B. Seo, B.C. Kim, S.K. Kim, C.-S. Song, M.B. Gu, Highly sensitive sandwich-type SPR based detection of whole H5Nx viruses using a pair of aptamers, Biosens. Bioelectron. 86 (2016) 293–300.
[19] J.-W. Park, S.J. Lee, E.-J. Choi, J. Kim, J.-Y. Song, M.B. Gu, An ultra-sensitive detection of a whole virus using dual aptamers developed by immobilization-free screening, Biosens. Bioelectron. 51 (2014) 324–329.
[20] N.H.A. Raston, M.B. Gu, Highly amplified detection of visceral adipose tissue-derived serpin (vaspin) using a cognate aptamer duo, Biosens. Bioelectron. 70 (2015) 261–267.
[21] S. Xie, S.P. Walton, Development of a dual-aptamer-based multiplex protein biosensor, Biosens. Bioelectron. 25 (2010) 2663–2668.
[22] A. Sosic, A. Meneghello, A. Antognoli, E. Cretaio, B. Gatto, Development of a multiplex sandwich aptamer microarray for the detection of VEGF165 and thrombin, Sensors 13 (2013) 13425–13438.
[23] B. Gorovits, S.C. Alley, S. Bilic, B. Booth, S. Kaur, P. Oldfield, S. Purushothama, C. Rao, S. Shord, P. Siguenza, Bioanalysis of antibody–drug conjugates: american association of pharmaceutical scientists antibody–drug conjugate working group position paper, Bioanalysis 5 (2013) 997–1006.

[24] L. Mao, Y. Liu, S. Yang, Y. Li, X. Zhang, Y. Wei, Recent Advances and Progress of Fluorescent Bio-/chemosensors Based on Aggregation-Induced Emission Molecules, Dyes Pigments (2018).
[25] X. Zhang, K. Wang, M. Liu, X. Zhang, L. Tao, Y. Chen, Y. Wei, Polymeric AIE-based nanoprobes for biomedical applications: recent advances and perspectives, Nanoscale 7 (2015) 11486–11508.
[26] Q.-y. Cao, R. Jiang, M. Liu, Q. Wan, D. Xu, J. Tian, H. Huang, Y. Wen, X. Zhang, Y. Wei, Microwave-assisted multicomponent reactions for rapid synthesis of AIE-active fluorescent polymeric nanoparticles by post-polymerization method, Mater. Sci. Eng. C 80 (2017) 578–583.
[27] R. Jiang, H. Liu, M. Liu, J. Tian, Q. Huang, H. Huang, Y. Wen, Q.-y. Cao, X. Zhang, Y. Wei, A facile one-pot Mannich reaction for the construction of fluorescent polymeric nanoparticles with aggregation-induced emission feature and their biological imaging, Mater. Sci. Eng. C 81 (2017) 416–421.
[28] H. Huang, D. Xu, M. Liu, R. Jiang, L. Mao, Q. Huang, Q. Wan, Y. Wen, X. Zhang, Y. Wei, Direct encapsulation of AIE-active dye with β cyclodextrin terminated polymers: self-assembly and biological imaging, Mater. Sci. Eng. C 78 (2017) 862–867.
[29] J. Chen, M. Liu, Q. Huang, L. Huang, H. Huang, F. Deng, Y. Wen, J. Tian, X. Zhang, Y. Wei, Facile preparation of fluorescent nanodiamond-based polymer composites through a metal-free photo-initiated RAFT process and their cellular imaging, Chem. Eng. J. 337 (2018) 82–90.
[30] U.D. Kamaci, M. Kamaci, A. Peksel, Poly (azomethine-urethane) and zeolite-based composite: fluorescent biosensor for DNA detection, Spectrochim. Acta A Mol. Biomol. Spectrosc. 212 (2019) 232–239.
[31] Y. Lan, G. Qin, Y. Wei, C. Dong, L. Wang, Highly sensitive analysis of tetrodotoxin based on free-label fluorescence aptamer sensing system, Spectrochim. Acta A Mol. Biomol. Spectrosc. 219 (2019) 411–418.
[32] X. Song, B. Fu, Y. Lan, Y. Chen, Y. Wei, C. Dong, Label-free fluorescent aptasensor berberine-based strategy for ultrasensitive detection of Hg2+ ion, Spectrochim. Acta A Mol. Biomol. Spectrosc. 204 (2018) 301–307.
[33] A.L. Ouellette, J.J. Li, D.E. Cooper, A.J. Ricco, G.T. Kovacs, in: Evolving Point-Of-Care Diagnostics Using Up-Converting Phosphor Bioanalytical Systems, ACS Publications, 2009.
[34] H. Zhu, F. Lu, X.-C. Wu, J.-J. Zhu, An upconversion fluorescent resonant energy transfer biosensor for hepatitis B virus (HBV) DNA hybridization detection, Analyst 140 (2015) 7622–7628.
[35] Y. Zhao, H. Wang, P. Zhang, C. Sun, X. Wang, X. Wang, R. Yang, C. Wang, L. Zhou, Rapid multiplex detection of 10 foodborne pathogens with an up-converting phosphor technology-based 10-channel lateral flow assay, Sci. Rep. 6 (2016), 21342.
[36] A. Sedlmeier, A. Hlaváček, L. Birner, M.J. Mickert, V. Muhr, T. Hirsch, P.L. Corstjens, H.J. Tanke, T. Soukka, H.H. Gorris, Highly sensitive laser scanning of photon-upconverting nanoparticles on a macroscopic scale, Anal. Chem. 88 (2016) 1835–1841.
[37] J. Lv, S. Zhao, S. Wu, Z. Wang, Upconversion nanoparticles grafted molybdenum disulfide nanosheets platform for microcystin-LR sensing, Biosens. Bioelectron. 90 (2017) 203–209.
[38] Z. Li, Y. Zhang, An efficient and user-friendly method for the synthesis of hexagonal-phase NaYF4: Yb, Er/Tm nanocrystals with controllable shape and upconversion fluorescence, Nanotechnology 19 (2008), 345606.
[39] K.W. Krämer, D. Biner, G. Frei, H.U. Güdel, M.P. Hehlen, S.R. Lüthi, Hexagonal sodium yttrium fluoride based green and blue emitting upconversion phosphors, Chem. Mater. 16 (2004) 1244–1251.
[40] T. Soukka, T. Rantanen, K. Kuningas, Photon upconversion in homogeneous fluorescence-based bioanalytical assays, Ann. N. Y. Acad. Sci. 1130 (2008) 188–200.
[41] N.H.A. Raston, V.-T. Nguyen, M.B. Gu, A new lateral flow strip assay (LFSA) using a pair of aptamers for the detection of Vaspin, Biosens. Bioelectron. 93 (2017) 21–25.
[42] J. Zhou, Z. Liu, F. Li, Upconversion nanophosphors for small-animal imaging, Chem. Soc. Rev. 41 (2012) 1323–1349.
[43] H.S. Mader, P. Kele, S.M. Saleh, O.S. Wolfbeis, Upconverting luminescent nanoparticles for use in bioconjugation and bioimaging, Curr. Opin. Chem. Biol. 14 (2010) 582–596.
[44] R.B. Liebherr, T. Soukka, O.S. Wolfbeis, H.H. Gorris, Maleimide activation of photon upconverting nanoparticles for bioconjugation, Nanotechnology 23 (2012), 485103.
[45] M. Fathil, M.M. Arshad, S.C. Gopinath, U. Hashim, R. Adzhri, R. Ayub, A. Ruslinda, A. Azman, M. Zaki, T.-H. Tang, Diagnostics on acute myocardial infarction: cardiac troponin biomarkers, Biosens. Bioelectron. 70 (2015) 209–220.
[46] J.-C. Boyer, F.C. Van Veggel, Absolute quantum yield measurements of colloidal NaYF 4: Er3+, Yb3+ upconverting nanoparticles, Nanoscale 2 (2010) 1417–1419.
[47] D.E. Achatz, R. Ali, O.S. Wolfbeis, Luminescent chemical sensing, biosensing, and screening using upconverting nanoparticles, in: Luminescence Applied in Sensor Science, Springer, 2010, pp. 29–50.
[48] S. Wilhelm, T. Hirsch, W.M. Patterson, E. Scheucher, T. Mayr, O.S. Wolfbeis, Multicolor upconversion nanoparticles for protein conjugation, Theranostics 3 (2013) 239.